ISSN1027-5495. Functional Materials, 31, No.4 (2024), p. 474-483
doi:http://dx.doi.org/10.15407/fm31.04.474

Peculiarities of transformations in systems of coordination nitrate precursors of rare earth elements and lithium during the formation of polyfunctional oxide materials

O.G. Dryuchko[1], V.V. Soloviev[2], N.V. Solovieva[3], O.V. Shefer[1], N.V. Bunyakina[1], M.V. Moskalenko[1], N.V. Yermilova[1]

[1] National University "Yuri Kondratyuk Poltava Polytechnic", 24 Pershotravneva Avenue, 36011, Poltava, Ukraine
[2] Poltava V.G. Korolenko National Pedagogical University, 2 Ostrohradskyi Street, 36003, Poltava, Ukraine
[3] Poltava State Medical University, 23 Shevchenko Street, 36011, Poltava, Ukraine

Received July 7, 2024

The article summarizes information important for practical use on the conditions of formation, composition, structure, forms of Ln coordination polyhedra, type of ligand coordination, and characteristic properties of lithium coordination nitrates of rare earth elements of the cerium subgroup of the isostructural series $Li_3[Ln_2(NO_3)_9]\cdot 3H_2O$ (Ln – La–Nd) (predecessors of promising modern multifunctional materials). The obtained data (as primary information) can serve as the basis for identifying, monitoring the phase state of processing objects in the preparatory stages; selection of criteria for the compatibility of components in the formation of single-layer and layered nanostructured oxide systems of lanthanides and transition elements with the structure of defective perovskite, garnet in the form of powders, thick films, bulk ceramics; development of various combined methods of their activation and establishment of technologically functional dependencies; controlled modification of the properties of the target product; optimization of synthesis modes of lithium-conducting systems such as electrodes of rechargeable batteries, electrolyte membranes and sensors, elements and instrument structures of modern telecommunications systems.

Keywords: lithium coordination lanthanide nitrates, formation conditions, crystal structure, characteristic properties, modification of titanate characteristics, lithium-conducting solid electrolytes.

Особливості перетворень у системах координаційних нітратних прекурсорів рідкісноземельних елементів і літію при формуванні поліфункціональних оксидних матеріалів. *О.Г. Дрючко, В.В. Соловйов, Н.В. Соловйова, О.В. Шефер,Н.В. Бунякіна, М.В. Москаленко, Н.В. Єрмілова*

Узагальнено важливі для практичного використання відомості про літієві координаційні нітрати рідкісноземельних елементів церієвої підгрупи ізоструктурного ряду $Li_3[Ln_2(NO_3)_9]\cdot 3H_2O$ (Ln – La–Nd) – прекурсори перспективних сучасних багатофункціональних матеріалів – щодо умов їх утворення й існування, природи хімічного зв'язку, складу, будови, форми координаційних поліедрів Ln, типу координації ліганд, функціональних властивостей. Одержані дані (як первинна інформація) є основою для виявлення, ідентифікації, контролю фазового стану об'єктів перероблення у підготовчих стадіях, вибору критеріїв сумісності складових при формуванні одношарових

і шаруватих наноструктурованих оксидних систем лантаноїдів і перехідних елементів різного призначення зі структурою дефектного перовскіта, граната у вигляді порошків, товстих плівок, об'ємної кераміки; розроблення різних комбінованих способів їх активації та встановлення технологічно-функціональних залежностей; керованого модифікування властивостей одержуваних цільових продуктів; оптимізації регламентів синтезу літій-провідних систем як електродів акумуляторів, що перезаряджуються, електролітних мембран і сенсорів, елементів і приладових структур сучасних систем телекомунікації.

1. Introduction

The great attention to complex oxides with a defective perovskite structure (ABO_3) (Li,La)TiO_3, $Li_{3x}La_{2/3-x}Y_{1/3-2x}TiO_3$ [1-6] and based on garnet-type $Li_5La_3M_2O_{12}$ (M – Nb, Ta) [7-9] is due to the peculiarity of the A-deficient crystal lattice: the presence of a sufficient number of vacancies in the basic structures, ensuring the free migration of charge carriers – lithium ions, and conduction channels through which ion transport occurs. These structural features open up wide possibilities for modifying the properties of complex oxides based on cationic substitutions and creating vacancies in cationic or anionic sublattices in order to achieve both high ionic conductivity and fast ion transport.

It was also established that partial heterovalent substitutions in the sublattice of rare earth elements can affect the phonon range [6]. This allows changing the properties of materials from ionic conductors to UHF (microwave) dielectrics and ferroelectric semiconductors [10].

This approach [11] allows creating lithium-conducting materials with high conductivity at room temperature $\sigma \sim 10^{-3}$ Ω/cm). Such systems can be used as solid-electrolyte membranes, electrodes in rechargeable lithium batteries and electrochromic devices, in electrochemical sensors, and also to develop materials on their basis [10] with relatively high permittivity, electrical quality factor, thermal stability of electrophysical properties in the microwave range for elements and devices in modern telecommunication systems. Lithium-conducting multicomponent oxides have a complex structure, and the synthesis of nanocrystalline materials is a difficult scientific and technological task.

The structure of such multicomponent oxide materials is presented in Fig. 1 [1].

The multicomponent oxide crystallizes in the strong perovskite-type structure consisting of octahedral TiO_6 framework stabilized by La atoms and having a large number of vacancies in unoccupied positions, which can be involved in the storage and transport of Li^+ [5]. In the refined structure there are two unequal positions of 'rich' and 'poor' La, alternately located along the *c* axis. It was established that the ionic conductivity of LLTO mainly depends on the size of the cation ion in the 'A' position (La or rare earth, alkali or alkaline earth), the concentration of lithium ions and vacancies, as well as the nature of the B–O bond.

According to research results [11], perovskites of $Li_{0.5}La_{0.5}TiO_3$ structure synthesized using solid-phase reactions, are promising, highly efficient family of anode materials for high-speed lithium-ion batteries [12]. With an average potential of about 1.0 V compared to Li^+/Li, this anode exhibits a high specific capacity of 225 mAh/g and withstands 3000 reverse phase transition cycles. Without reducing the particle size to micro- and nanoscale, its speed characteristics exceed those of commercial nanostructured $Li_4Ti_5O_{12}$.

Although these materials have been widely studied in bulk form, there are no data on the synthesis and characterization of corresponding film materials. This is why the synthesis of lithium-conducting materials in the form of films that can be used as a solid electrolyte for solid-state batteries to power autonomous devices in telecommunications systems, medicine, and the automotive industry is relevant.

Thin films are produced mainly using physical synthesis methods, such as radio frequency (RFS) and magnetron sputtering (RFMS); while thick films are produced using 'screen printing', laser structuring, deposition using photosensitive paste and 'tape casting'. Each method has its own characteristics and areas of most effective use. According to [13], the 'tape casting' method (casting, a type of "soft chemistry" solution) is optimal to obtain thick films of thickness more than 10 μm.

Currently, soft chemistry methods are being developed using liquid multicomponent nitrate systems [14, 15], which make it possible to prevent lithium losses and reproduce single-phase samples with controlled ordering of cations and vacancies in the crystallographic positions of perovskite structures at low temperatures. The mechanism of formation of nanoparticles under such conditions is quite complex from a

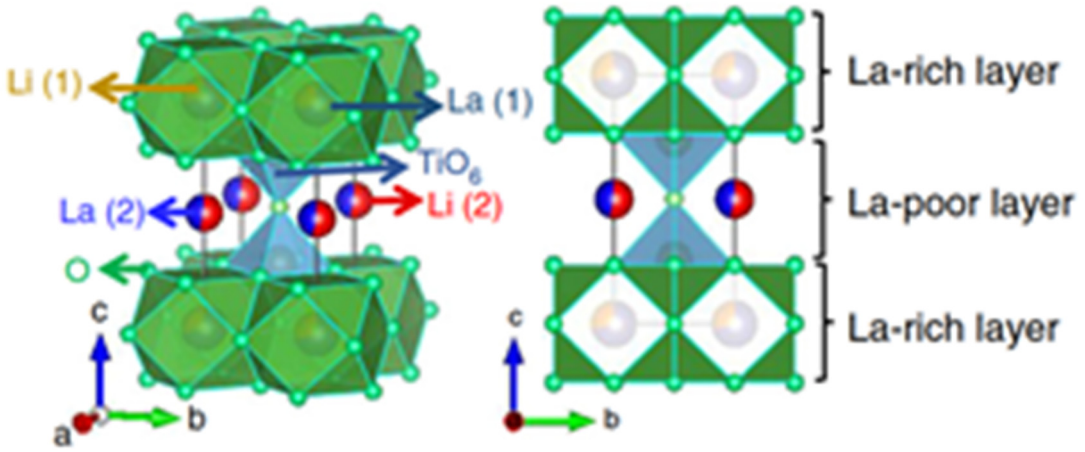

Fig. 1. Schematic representation of the crystal structure $Li_{0.5}La_{0.5}TiO_3$ (LLTO) [1]

physicochemical point of view and may include parallel processes such as hydration (solvation), association, complexation, formation and transformation of heterophases, the patterns of which have been poorly studied.

This study was initiated by available information on the status and possible directions for improving technologies for creating oxide REE-containing functional materials, methods for activating processes and existing requirements for their stability and reproducibility.

The purpose of this work is a fundamental study of cooperative processes occurring during the production of oxide functional materials containing rare earth elements; at the preparatory stages we use nitrates of elements with different electronic structures, and we also search for possible methods of influencing liquid-phase and solid-phase systems based on thermal activation, reproducing their structure-sensitive characteristics.

To assess the possibility of controlling these processes and obtaining materials with specified properties using a set of physical and chemical methods, it is necessary:

a) to study the chemical interactions and phase equilibria in model water-salt systems $LiNO_3 – Ln(NO_3)_3 – H_2O$ (Ln – Y, La – Lu) in the temperature range of 25 – 100°C;

b) construct polythermal solubility diagrams of the systems; determine the concentration and temperature limits of crystallization of the starting substances and detected complex compounds;

c) to find out the optimal growth conditions and synthesize coordination nitrates of rare earth elements and lithium, study their properties and confirm their individuality;

d) to establish the patterns of dependence of the quantity, composition, and properties of coordination nitrates formed in the systems under study on the nature of Ln^{3+} complex-forming ion and the conditions of formation.

2. Experimental

To clarify the nature of the chemical behavior of structural components and phase equilibria in the studied water-salt systems as precursors of multicomponent functional materials containing REE, we used the solubility method described in our previous works [16, 17] under isothermal conditions (at 25, 50, 65, 100 °C) in the temperature range of the existence of solutions in full concentration ratios. The phase equilibrium was achieved within 2-3 days. Hydrated and anhydrous nitrates of the specified elements, marked as 'pure for analysis', were used as initial salts.

Chemical analysis of the "residues" of the liquid and solid phases for the content of Ln^{3+} and nitrogen was carried out. The content of Ln^{3+} was determined trilonometrically in the presence of xylenol orange as an indicator (acetate buffer solution, pH=5–6) [18]; nitrogen was determined by the distillation method [19]; the content of Me^+ ions was calculated based on the difference between the total content of nitrates and the partial dry residue. The obtained data for individual ions were converted to the salt content and displayed on solubility diagrams according to the principle of correspondence. The graphical representation of the composition of the resulting solid phases was carried out according to the Schreinemakers method [20]. For characterization, chemical, crystal

Table 1a . Conditions for the formation of lithium double lanthanide nitrates of the cerium subgroup in $LiNO_3 – Ln(NO_3)_3 – H_2O$ (Ln – La – Sm) systems at 25 – 100 °C

t, °C	Systems / Isotherm points			Composition of points on the phase diagram, wt. %				
				La	Ce	Pr	Nd	Sm
25	A_1	Solubility $LiNO_3$, mass. %	47.66					
	B_1^I	Figurative (eutonic) point	$LiNO_3$	31.92	31.09	35.84	35.45	31.94
			$Ln(NO_3)_3$	31.86	32.03	26.65	28.07	30.07
	B_1^{II}	Figurative point	$LiNO_3$	19.54	20.49	24.13	28.28	
			$Ln(NO_3)_3$	47.96	47.08	41.69	37.63	
	C_1	Solubility $Ln(NO_3)_3 \cdot 6H_2O$, mass. %		58.92	59.05	59.01	58.89	59.22
50	A_2	Solubility $LiNO_3$, mass. %	63.80					
	B_2	Eutonic point	$LiNO_3$	23.29	22.87	21.93	21.48	24.90
			$Ln(NO_3)_3$	53.61	53.89	54.28	54.35	46.96
	C_2	Solubility $Ln(NO_3)_3 \cdot 6H_2O$, mass %		65.79	66.62	66.64	66.16	65.59
100	A_3	Solubility $LiNO_3$, mass %	67.28					
	D_1	Transitional (eutonic) point	$LiNO_3$	27.11	26.84	24.09	24.03	17.56
			$Ln(NO_3)_3$	53.35	54.35	54.66	54.68	67.31
	Compound F_1	Component ratio		3:2:3	3:2:3	3:2:3	3:2:3	
		Solution behaviour		cong.	cong.	cong.	cong.	
	G	Eutonic point	$LiNO_3$	9.92	9.76	8.73	9.68	
			$Ln(NO_3)_3$	71.03	71.45	72.20	72.51	

optical, X-ray phase, X-ray structural, IR-spectroscopic, thermographic and other methods were used.

The crystal-optical study was carried out by the immersion method using a MIN-8 microscope. Phase analysis was performed by the "powder" method on a DRON-3M diffractometer (Cu-K_α radiation, Ni filter). Diffraction patterns were interpreted using the JCPDS PDF file. The symmetry, unit cell parameters, and intensity of diffraction reflections from single crystals were determined using an automatic X-ray single-crystal diffractometer CAD - 4F "Enraf - Nonius" (Mo K_α - radiation, graphite monochromator; ω / 2θ - method). All calculations for the determination and refinement of atomic structures were performed using the SHELX, XTL – SM, AREN crystallographic software packages. The IR absorption spectra of the synthesized compounds in the region of 400–4000 cm^{-1} were recorded on a UR – 20 spectrophotometer using a standard vaseline oil suspension technique. Thermograviometric analysis was carried out in the range of 20 °C to 1000 °C in air at a heating rate of 10 degrees/ min on a Q – 1500 D derivatograph and the developed device for DTA.

3. Results and discussion

The obtained experimental data are summarized in Table 1a, 1b and used for graphical interpretation of the research results (see Fig. 2. Solubility polytherms $LiNO_3 – Ln(NO_3)_3 – H_2O$ (Ln – La – Nd)).

The exchange interactions between the structural components with the formation

Table 16. Data on the study of phase equilibria in systems $LiNO_3 – Ln(NO_3)_3 – H_2O$ (Ln – Y, Gd – Lu) at 25, 50, 100 °C

t, °C	Systems: Isotherm points			Composition of points on the phase diagram, mass %: Y	Gd	Tb	Dy	Ho	Er	Tm	Yb	Lu
25	A_1	$LiNO_3$, solutability mass %	47.7									
	B_1	Eutonic point	$LiNO_3$	31.4	32.7	31.8	31.9	31.3	31.4	25.9	19.2	18.8
			$Ln(NO_3)_3$	30.6	30.5	32.5	33.5	34.4	34.5	41.4	51.6	53.2
	C_1	$Ln(NO_3)_3$ solutability and its hydration in solid, mass %		59.26	59.55	60.25	62.45	65.25	66.15	68.25	70.14	71.74
50	A_2	$LiNO_3$, solutability mass %	63.8									
	B_2	Eutonic point	$LiNO_3$	31.2	38.1	33.6	34.5	33.8	32.3	21.6	22.4	22.6
			$Ln(NO_3)_3$	40.7	37.3	38.4	39.5	43.3	45.2	53.7	56.5	56.9
	C_2	$Ln(NO_3)_3$ solutability and its hydration in solid, mass %		63.96	65.75	66.45	67.75	69.05	70.45	73.05	75.24	76.34
100	A_3	$LiNO_3$, solutability mass %	67.3									
	B_3	Eutonic point	$LiNO_3$	16.8	15.9	16.2	16.3	16.2	16.5	16.2	15.3	15.0
			$Ln(NO_3)_3$	64.5	67.9	68.3	68.9	68.5	67.0	67.5	68.9	69.0
	C_3	$Ln(NO_3)_3$ solutability and its hydration in solid, mass %					74.84	75.94	75.34	76.14	81.34	81.63

of new anionic coordination compounds of lanthanides were discovered in the range of 25-100°C. Their number (four), composition, possible types of compounds, concentration limits of crystallization of phases coexisting in specific systems and the nature of their solubility were studied, and solubility phase diagrams were constructed. The concentration boundaries of saturated solutions from which the coordination Ln nitrates are released correspond to the composition of the invariant points of the solubility isotherms. All of them are synthesized in the form of single crystals. Their individuality was confirmed and a number of their properties have been systematically studied.

Crystallization fields were found in the studied water-salt systems of nitrates of lithium and rare earth elements of the cerium subgroup:

– initial nitrates:

1) lithium (crystalline hydrate $LiNO_3 \cdot 3H_2O$ at t ~ 30°C, anhydrous $LiNO_3$ at t > 30°C) and 2) lanthanides La – Sm (hexahydrate $Ln(NO_3)_3 \cdot 6H_2O$ at t<68°C, at higher temperatures – crystalline hydrate forms of the indicated lanthanides are unstable and are in a liquid state);

– coordination compounds $Li_3[Ln_2(NO_3)_9] \cdot 3H_2O$ (Ln–La – Nd, congruently soluble in water), were discovered, which are released from solutions at t>65°C. (Probably, the region of existence of the similar compound in the samarium system in the isothermal region of 100°C is very narrow).

The B_1^I - B_1^{II} gap in the middle part of the solubility isotherms (25 °C) of the La - Sm ternary systems indicates that in this region of concentration ratios there are components in a liquid state due to the release of hydrated lithium and lanthanide nitrates in quantities sufficient for a “solid residue”. Systems based on compounds of rare earth elements of the yttrium subgroup are characterized by the existence of crystallization fields of only initial substances with different resistance to hydration, and Y, Gd – Lu systems belong to the eutonic type.

The features of the atomic-crystalline structure of identified lithium complex nitrates of lanthanides [21], crystallizing within the $P2_13$ group, and a number of their properties were studied (Table 2). The authors of the work established the characteristic X-ray diffraction pa-

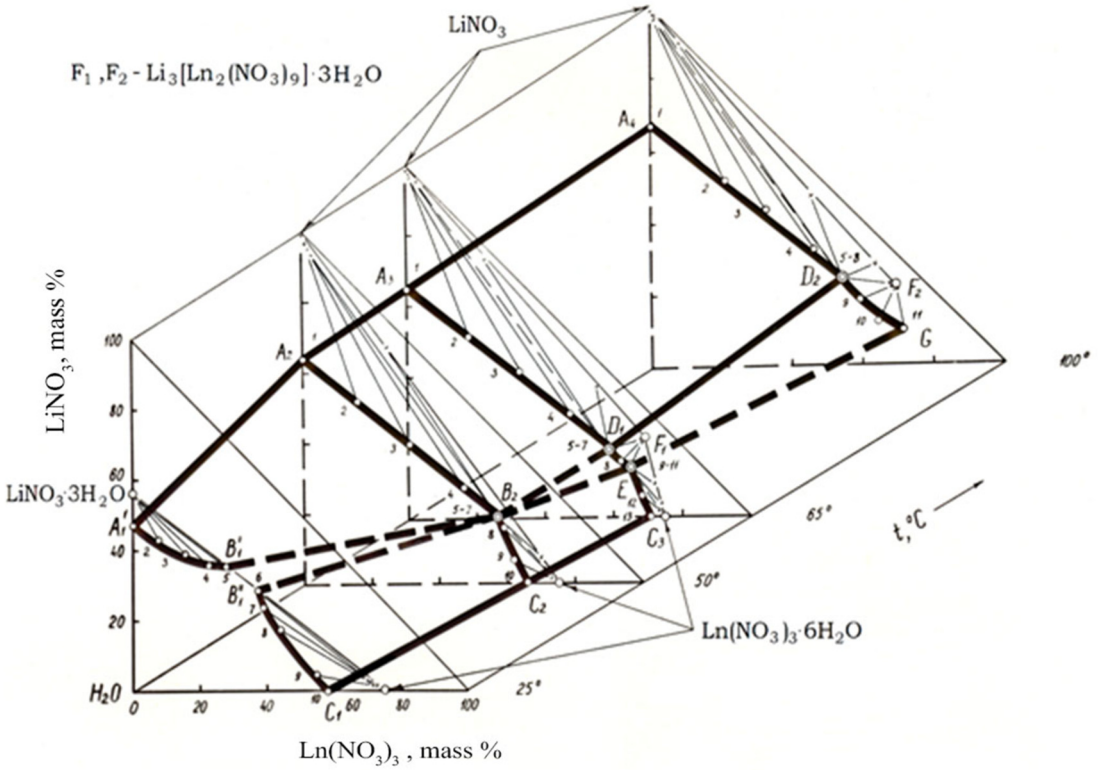

Fig. 2. Solubility polytherm of the system $LiNO_3$ – $Ln(NO_3)_3$ – H_2O (Ln – La ÷ Nd)

Table 2 – Crystallographic characteristics and the possibility (based on symmetrical representations) of manifestation of properties in crystals of some coordination lithium nitrates of rare earth elements [21]

Compounds	Syngonia	Point group	Space group	Z	Cell parametres, Å	V, Å^3	Properties
$Li_3[La_2(NO_3)_9]\cdot 3H_2O$	кубіч.	23	$P2_13$	4	13.354(2)	2381.4	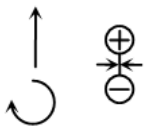
$Li_3[Nd_2(NO_3)_9]\cdot 3H_2O$				4	13.220(1)	2308.4	

rameters of newly formed phases for their identification and detection during stage transformations (see Table 3, Fig. 3); also, the established nature and patterns of thermal transformations of compounds in the temperature range of 25–1000 °C make it possible to predict their thermal stability and model the behavior of technological objects under similar conditions.

In a representative of the isostructural type of lithium-neodymium compounds, the Nd atoms are distributed over two individual positions on the three-order axes. Their coordination polyhedra are somewhat distorted and icosahedral, composed of oxygen atoms of six bidentately attached nitrate groups (Fig. 4).

The icosahedra around Nd1 and Nd2 are constructed differently. The difference is the distribution of the shortened ribs. The difference in the structure of polyhedra can be explained by considering specific NO_3 ligands. The structure contains three nonequivalent sets of nitrate groups characterized by certain features of bonds with Nd and Li atoms and clearly reflected in Fig. 5.

Table 3 - X-ray data on lithium coordination neodymium nitrate

$Li_3[Nd_2(NO_3)_9]\cdot 3H_2O$					
d, Å	I/I_0, %	d, Å	I/I_0, %	d, Å	I/I_0, %
8.36	30	3.90	40	2.135	49
7.64	77	3.56	26	2.111	43
6.68	13	3.32	19	2.013	19
6.00	38	3.22	47	1.979	19
5.75	79	2.978	34	1.944	28
5.42	98	2.772	19	1.931	26
5.26	74	2.617	28	1.855	15
4.76	51	2.545	43	1.778	15
4.64	100	2.385	21	1.726	28
4.35	43	2.328	17	1.708	34
4.19	47	2.305	23	–	–
3.94	51	2.226	19	–	–

Note: d, Å – interplanar distances; I/I_0, % – relative intensities of reflections

Similar to all compounds previously discovered in water-salt systems [17], in cases where water is not included in the coordination sphere of the Ln-complexing agent and coordination saturation of the complex occurs without its participation, the nitrate group of one of the nitrogen atoms (N1) performs the functions of two independent complexing agents, and its capacious oxygen atoms bind the $[Nd(NO_3)_6]^{3-}$ complexes into a three-dimensional framework

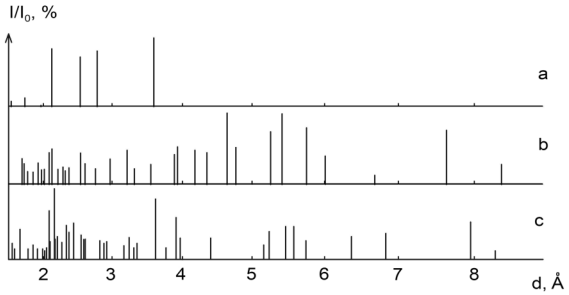

Fig. 3 – X-ray diffraction patterns a) $LiNO_3$; b) $Li_3[Nd_2(NO_3)_9]\cdot 3H_2O$; c) $Nd(NO_3)_3\cdot 6H_2O$

with the formula $[Nd_2(NO_3)_9]^{3-}{}_{\infty\,\infty\,\infty}$. The projection of the $Li_3[Nd_2(NO_3)_9]\cdot 3H_2O$ structure onto the *'xy'* plane is shown in Fig. 6a. For convenience, Fig. 6b schematically shows the framework of the $Li_3[Nd_2(NO_3)_9]\cdot 3H_2O$ structure in the same projection. The letters A–D in both figures indicate the corresponding Nd atoms.

The Li atoms are placed in large channels and include four oxygen atoms in their coordination region. Their coordination polyhedra are characteristic flattened tetrahedra, each of which is formed by oxygen atoms of water and nitrate groups N2 and N3. Thus, in lithium-neodymium nitrate of the $Li_3[Nd_2(NO_3)_9]\cdot 3H_2O$ composition the Li atom providing additional bonds between rare-earth complexes, contributes to the presence of intermolecular water in the structure, and also causes some difference in the structure of rare-earth icosahedra, which, in turn, perform the main structure-forming function in rare earth nitrate compounds.

It was established in [17] that if the structure of nitrate compounds of lanthanides of the cerium subgroup is based on polynuclear complexes,

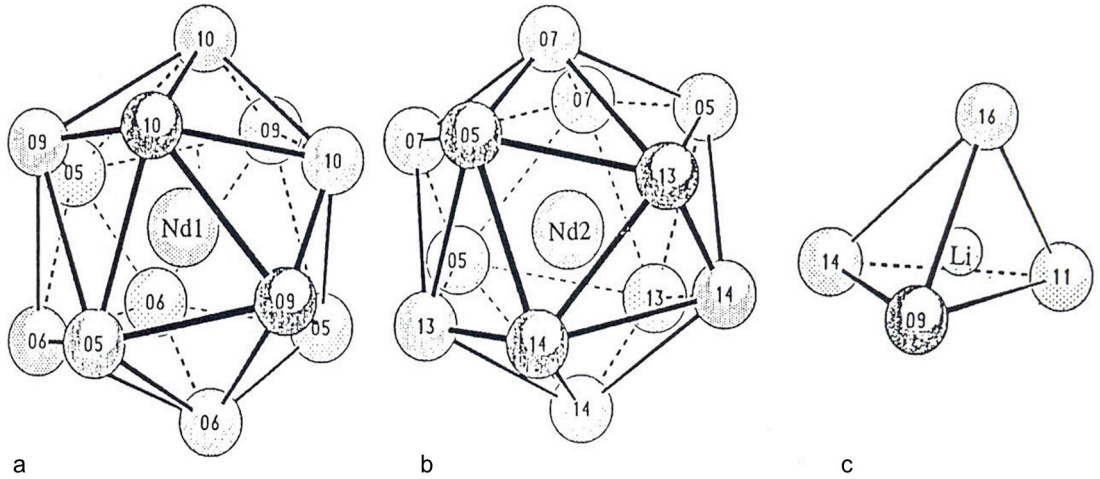

Fig. 4 - Coordination polyhedra of Nd 1(a), Nd 2(b) and Li(c) atoms in the structure of $Li_3[Nd_2(NO_3)_9]\cdot 3H_{2O}$

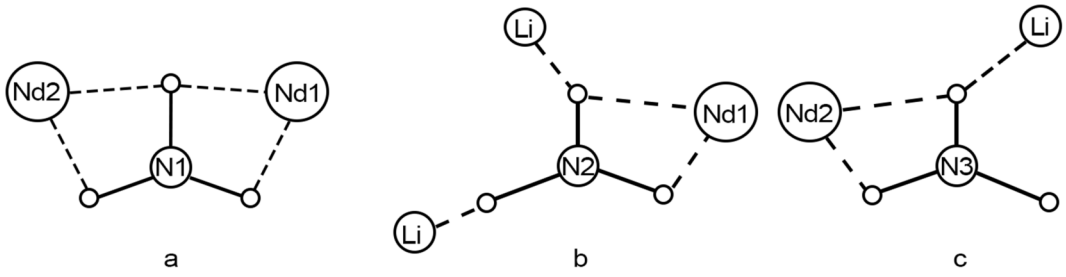

Fig. 5 – The schematic representation of 3 nonequivalent sets of nitrate groups in the structure of $Li_3[Nd_2(NO_3)_9]\cdot 3H_2O$

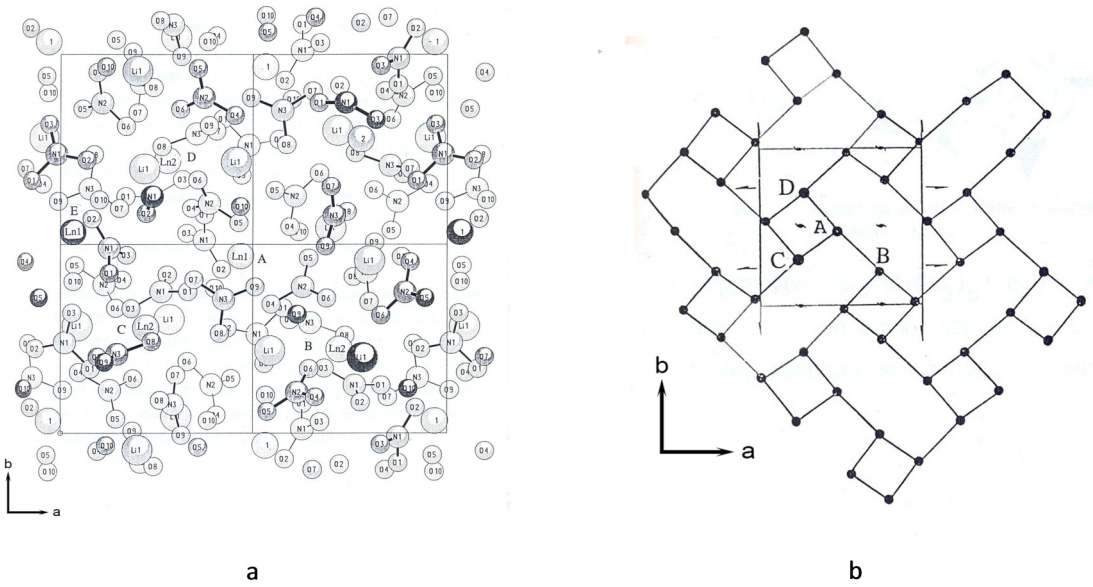

Fig. 6 – Projection of the structure of $Li_3[Nd_2(NO_3)_9]\cdot 3H_2O$ onto the *xy* plane (a) and its schematic representation (b), [21]

then water in them is either completely absent or present only in crystals of $Na_2[Ln(NO_3)_5]\cdot H_2O$ (Ln – La–Sm), $Rb_5[Ln_2(NO_3)_{11}]\cdot H_2O$ (Ln – Pr–Sm), $Me_3[Ln_2(NO_3)_9]\cdot nH_2O$ (Me – Li n=3, Me – K, Rb, NH_4^+ n=0, 1 Ln – La–Sm).

It is known that the nitrate group is a planar polyanion with a third-order symmetry axis. When it is coordinated by another atom, its geometry can become distorted. In rare earth nitrates, the Ln^{3+} ion is usually located in the same plane with nitrate groups [22, 23]. This configuration corresponds to the minimum energy of component interaction. This feature of systems of nitrate precursors with the participation of Ln^{3+} and Li^+, Na^+, K^+, NH_4^+, Rb^+ according to the authors [22, 23] is a favorable prerequisite for the association of components during the formation of complex oxide phases of desired products with layered and chain packing upon heating.

The obtained results suggest that the process of decomposition of crystalline alkali rare earth nitrates in technological objects during thermal activation begins with the rupture of the alkaline metal-oxygen bond. This is confirmed by the results of thermographic studies of the specified compounds in the temperature range of 25–1000 °C.

Using a derivatograph and a developed setup for differential thermal analysis, the thermal stability of a representative of the isostructural series of lithium-lanthanide nitrates of the cerium subgroup, $Li_3[Nd_2(NO_3)_9]\cdot 3H_2O$, was studied. In the thermogram of the compound (Fig. 7), in addition to the output state corresponding to the formation of anhydrous binary nitrate and thermolysis products at temperatures above 900 °C, two temperature ranges of mass stabilization are visible. Above 347-384 °C, intensive decomposition of the melt occurs with the release of nitrogen, hydrogen,

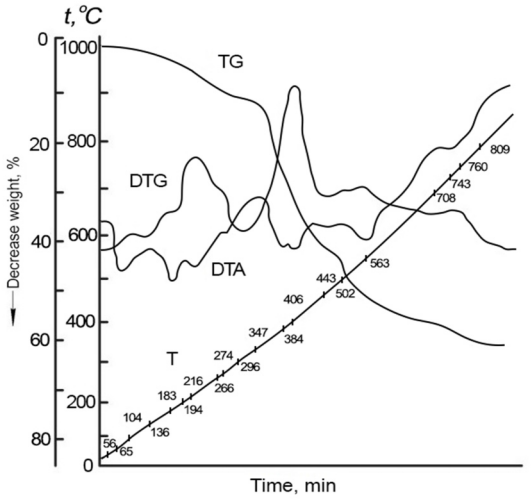

Fig. 7. Derivative diagrams for $Li_3[Nd_2(NO_3)_9]\cdot 3H_2O$. T – temperature curve; DTA – differential temperature curve; TG – thermogravimetric curve; DTG – differential thermogravimetric curve

and nitrogen oxides and a continuous change in the composition of the samples under study. The final products of thermal transformation depend on the composition of the initial coordination REE nitrate and the nature of the alkali metal present.

The derivatogram of $Li_3[Nd_2(NO_3)_9]\cdot 3H_2O$ shows a number of endothermic effects. The first three (65, 183, 216 °C) correspond to the process of dehydration of the trihydrate. At a temperature of 65 °C, partial melting occurs and at 183 °C, complete incongruent melting occurs in crystallization water. Subsequent thermal transformations including the completion of nitrogen evolution occur in the melt. On the TG curve at 274–347 °C, a mass stabilization interval is observed, corresponding to the composition of the melt of anhydrous lithium-neodium coordination nitrate.

This is confirmed by the chemical analysis. This behavior of the system is explained by the superposition of the thermal effects of dehydration and melting of $Li_3[Nd_2(NO_3)_9]$ due to the proximity of their temperature values and the inertia of the dehydration process. The decrease in the mass of decomposition products above 809 °C corresponds to the formation of $LiNdO_2$ a small amount of Li_2O and an Nd_2O_3 impurity, which is confirmed by X-ray diffraction (Table 4) and is consistent with the data of [24]. Lithium dioxoneodymate crystals belong to the α-$LiEuO_2$ structural type monoclinic system, space group $P2_1/c$; cell parameters, Å: a = 5.77, b = 6.09, c = 5.72 β=103°07; V = 200.7 Å^3.

Table 4 - X-ray phase analysis data on products of decomposition of lithium coordination nitrate neodymium at 960 °C

$Li_3[Nd_2(NO_3)_9]\cdot 3H_2O$					
d, Å	I/I_0, %	d, Å	I/I_0, %	d, Å	I/I_0, %
5.60	17	2.520	95	1.762	8
4.11	44	2.296	14	1.743	19
3.61	90	2.221	14	1.710	15
3.31	12	2.060	26	1.669	26
3.07	100	2.051	28	1.642	15
3.03	19	2.045	31	1.638	14
2.994	11	2.039	31	1.631	9
2.899	42	1.907	50	1.612	19
2.806	29	1.871	16	1.606	37
2.782	36	1.837	25	1.596	19
2.750	26	1.786	20	1.519	16
2.669	46	1.774	27	1.503	15

Note: d, Å – interplanar distances; I/I_0, % – relative intensities of reflections

The obtained empirical data on the atomic-crystalline structure, properties, nature and stages of thermal transformations of lithium coordination lanthanide nitrates play an important role in optimizing the technologies for the production of new multifunctional REE-containing materials; this promotes the development of innovations in various branches of industry, makes it possible to explain and predict the properties of intermediate phases and has both independent scientific and applied value.

The acquired knowledge has particular significance for the obtaining of nanostructured perovskite-like compounds of lanthanides and transition elements, solid solutions based on them (including titanium, described in [1–14], and others). This clarify the relationships between the preparation method and the variability of the activation method of the systems, phase composition, lattice parameters, specific surface area, morphology of the constituent particles, catalytic and photocatalytic activity of the samples in reactions of water decomposition to obtain hydrogen, decomposition of toxic organic substances, incomplete oxidation. This can significantly simplify the procedures for synthesizing target products when obtaining

other perovskite phases through ion exchange reactions.

4. Conclusions

A generalization of information on precursors of promising modern multifunctional materials $Li_3[Ln_2(NO_3)_9]\cdot 3H_2O$ (Ln – La–Nd), important for practical applications (conditions of their formation and existence, composition, structure, shapes of Ln coordination polyhedra, type of ligand coordination, functional properties) is carried out. The data obtained can be used as the basis for identifying, monitoring the phase state of processing objects in the preparatory stages, selecting criteria for the compatibility of components in the formation of single-layer and layered nanostructured oxide systems of lanthanides and transition elements with the structure of defective perovskite, garnet in the form of powders, thick films, bulk ceramics, development of various combined methods of their activation and establishment of technologically functional dependencies, controlled modification of the resulting desired product properties.

References

1. S. Stramare, V. Thangadurai, W. Weppner, *Chem. Mater.* **15**, 3974 (2003).
2. M. Nakayama, T. Usui, Y. Uchimoto et al., *J. Phys. Chem*. **B 109**, 4135 (2005).
3. V.M. Ishchuk, V.L. Cherginets, O.V. Demirskaya et al., *Ferroelectrics*, **298**, 135 (2004).
4. W.J. Kwon, H. Kim, K. Jung et al., *J. Mater. Chem*. **A 5**, 6257 (2017).
5. A. Belous, O. Yanchevskiy, O. V'yunov, *Chem. Mater*. **16**, 407 (2004).
6. A.G. Bilous, *Ukr. Khim. Zh*. **75** (7), 3 (2009).
7. O.M. Gavrilenko, *Ukr. Khim. Zh*. **70** (9), 31 (2004).
8. O.M. Gavrilenko, O.V. Pashkova, A.G. Bilous, *Ukr. Khim. Zh*. **71**(8), 73 (2005).
9. A. Ramzy, V. Thangadural, *ACS Applied Materials & Interfaces*. **2** (2), 385 (2010).
10. A.G. Bilous, *Ukr. Khim. Zh*. **74** (1), 3 (2008).
11. Zhang Lu, Zhang Xiaohua, Tian Guiying et al., *Nature Communications*. **11**, 3490, 1 (2020).
12. C. Hua, X. Fang, Z. Wang et al., *Electrochem. Commun*. **32**, 5 (2013).
13. S.D. Kobylyanska, B.O. Linyova, S.O. Solopan et al., *Ukr.Chem. J.,*. **81** (7), 25 (2015).
14. Jena Hrudananda, K.V. Govindan Kutty, *J. Mater. Sci*. **40**, 4737 (2005).
15. O.G. Dryuchko, D.O. Storozhenko, N.V. Bunyakina et al., Coll. of scientific works OJSC "UkrNDIV named after A.S. Bereznogo". - Kh.: Caravela, 110, 58 (2010).
16. O.G. Dryuchko, D.O. Storozhenko, N.V. Bunyakina et al., *Bulletin of the NTU "KhPI". Series: Chemistry, Chemical Technology and Ecology*, **38**(1269), 34 (2017).
17. O.G. Dryuchko, D.O. Storozhenko, N.V. Bunyakina et al., *Bulletin of the NTU "KhPI". Series: Chemistry, Chemical Technology and Ecology*, **39**(1315), 3 (2018).
18. A.I. Busev, V.G. Tiptsova, V.M. Ivanov, *Management on analytical chemistry of rare elements.* Moscov. Chemistry Publ. – 432 p. (1978).
19. A.P. Kreshkov, *Fundamentals of Analytical Chemistry. Quantitative analysis*. Moscov, Chemistry Publ., book. 2. - 480 p. (1976).
20. Ya.G. Goroshchenko, *Physical and Chemical Analysis of homogenous and heterogenous systems.* Kiev, Naukova dumka Publ. – 490 p. (1978).
21. A.G. Vigdorchik, Yu.A. Malinovskiy, A.G. Dryuchko et al., *Crystallography*, **36**(6), 1395 (1991).
22. B. Eriksson, *Chemical communication. Univ. of Stockholm*. 3, 1 (1982).
23. C.C. Addison, N. Logan, S.C. Wallwork et al., *Quart. Rev*. **25**, 289 (1971).
24. L.P. Shklover, I.F. Zakharchenko, L.M. Shkolnikova et al., *Journal inorganic chemistry*.**20** (7), 1759 (1975).